Multimodal change monitoring using multitemporal satellite images.

Datta, U.

U. Datta, "Multimodal change monitoring using multitemporal satellite images.," Proc. SPIE 11862, Image and Signal Processing for Remote Sensing XXVII, 118620M (12 September 2021); doi: 10.1117/12.2600099

Event: SPIE Remote Sensing, 2021, Online Only

Multimodal change monitoring using multitemporal satellite images

U. Datta

Norwegian Defence Research Establishment (FFI), Instituttveien 20, NO-2007 Kjeller.

ABSTRACT

The main objective of this study is to monitor the land infrastructure growth over a period of time using multimodality of remote sensing satellite images. In this project unsupervised change detection analysis using ITPCA (Iterated Principal Component Analysis) is presented to indicate the continuous change occurring over a long period of time. The change monitoring is pixel based and multitemporal. Co-registration is an important criteria in pixel based multitemporal image analysis. The minimization of co-registration error is addressed considering 8- neighborhood pixels. Comparison of results of ITPCA analysis with LRT (likelihood ratio test) and GLRT (generalized likelihood ratio test) methods used for SAR and MS (Multispectral) images respectively in earlier publications are also presented in this paper. The datasets of Sentinel-2 around 0-3 days of the acquisition of Sentinel-1 are used for multimodal image fusion. SAR and MS both have inherent advantages and disadvantages. SAR images have the advantage of being insensitive to atmospheric and light conditions, but it suffers the presence of speckle phenomenon. In case of multispectral, challenge is to get quite a large number of datasets without cloud coverage in region of interest for multivariate distribution modelling.

Keywords: ITPCA, Multimodal, SAR, Multispectral, Change detection, LRT, GLRT

1. INTRODUCTION

The infrastructure growth of land over a period of time using multisensor multitemporal remote sensing signal is the main objective in this study. The change detection in remote sensing involves comparison of the images taken of the same spatial region collected at different points in time [1]. Most of the change detection methods using remote sensing images are spectral based [2]. Bi-temporal change detection method is unable to indicate the continuous change occurring over a long period of time. To achieve this objective, the datasets over three years are considered for analysis. The remote sensing satellites orbiting earth continuously captures data in different parts of the electromagnetic spectrum with different spatial and spectral resolutions and coverage. This data acquisitions from multisensor remote sensing have different inherent advantages and disadvantages for change detection monitoring. As for example, while SAR imagery measures physical properties of the observed scene and can be acquired at all weather and at daylight/night conditions, multispectral imagery measures chemical characteristics and needs daylight without cloud coverage for monitoring. Multispectral data is much easier to interpret visually, whereas SAR data contains not only amplitude but also phase information, which enables a high-precision measurement of three-dimensional topography. SAR image suffers the presence of speckle phenomenon. The technique of change detection for remote sensing data has been developed with increase in the spatial resolution of remote sensing.

Remote sensing images obtained from different types of sensors carry distinct information and integration of this information can be more advantageous than information obtained from a single type of sensor. The fused remote sensing image is obtained by combining two or more geometrically registered geo-located images. The fusion techniques can be performed at three different processing levels such as pixel level, feature level and decision level. Remotely sensed images of multimodal sensor is an effective tool which is capable of providing extra information [3] in spatial and spectral resolution.

urmila.datta@ffi.no; phone +47 6380 7447; www.ffi.no/en

Image and Signal Processing for Remote Sensing XXVII, edited by Lorenzo Bruzzone,
Francesca Bovolo, Proc. of SPIE Vol. 11862, 118620M · © 2021 SPIE
CCC code: 0277-786X/21/$21 · doi: 10.1117/12.2600099

2. DATASET AND PREPROCESSING

The SAR datasets of Sentinel-1 Level-1 GRD (Ground Range Detected) data are obtained from Copernicus Open Access Hub [4]. The multispectral datasets of Sentinel-2 are also obtained from the same open source. The area called Stockholm Norvik Hamn is selected for infrastructure growth analysis. It is Sweden's harbor area. In this area, there is an ongoing project for building the harbor for rolling goods and containers at Norvikudden, outside Nynashamn. In addition to the harbor, a railway is also being connected to Nynasrailway network, and a construction group is building a logistics and business park adjacent to the harbor.

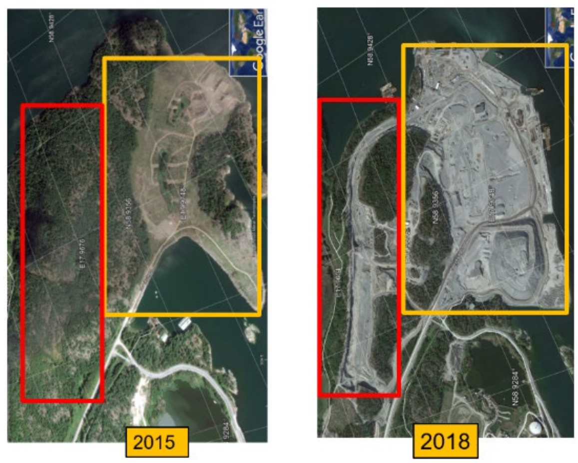

a b

Figure 2.1 Picture of Stockholm Norvik Hamn taken from google earth. The figure a) is taken in 2015 and the picture b) is taken in 2018.

In the figure 2.1 the picture marked 'a' is taken in the year 2015 and the second picture marked 'b' is taken in 2018. Visual inspection shows the change due to infrastructure growth. The Sentinel-1 GRD scene is composed of approximate square pixels. The multi-look processing results the final product with reduced speckle. The final product is the detected amplitude, but the phase information is lost. Before data analysis it is pre-processed using the SNAP software for further reduction of speckle noise and terrain correction [5] as shown in figure 2.2.

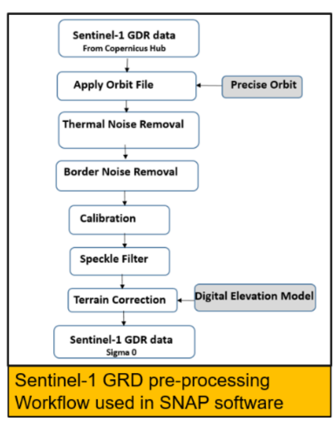

Figure 2.2 Sentinel-1 GRD preprocessing workflow used in snap software.

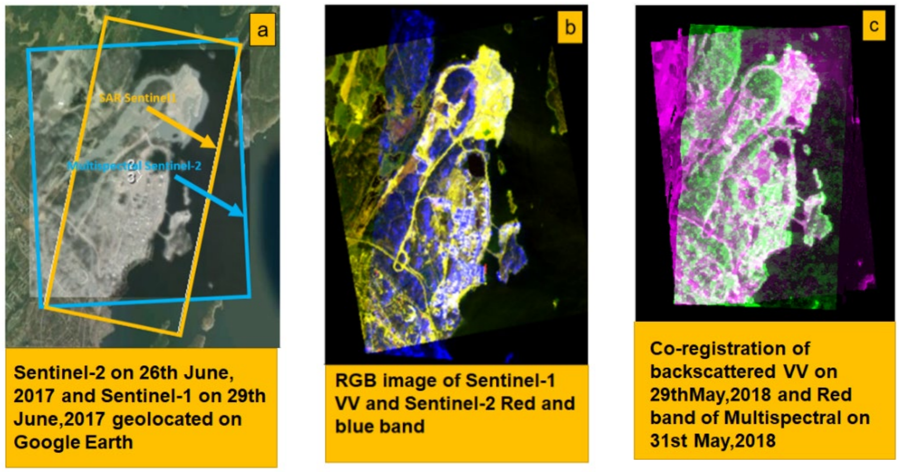

Figure 2.3 a) Sentinel-1 and Sentinel-2 geo-located border on Google earth, b) RGB image composed of Sentinel-1 VV, red and blue band of Sentinel-2, c) Co-registered VV band of Sentinel-1 and Sentinel-2 red band.

Datasets	Sentinel-2	Sentinel-1
Image Number	Date of acquisation	Date of acquisation
Image-1	04. 07. 2015	03.07.2015
Image-2	24. 07. 2015	22.07.2015
Image-3	13. 08. 2015	15.08.2015
Image-4	23. 08. 2015	20.08.2015
Image-5	06. 10. 2016	08.10.2016
Image-6	26. 06. 2017	29.06.2017
Image-7	06. 07. 2017	04.07.2017
Image-8	01. 09. 2017	02.09.2017
Image-9	29. 05. 2018	31.05.2018
Image-10	08. 07. 2018	11.07.2018
Image-11	31. 07. 2018	30.07.2018
Image-12	17. 08. 2018	16.08.2018
Image-13	19. 09. 2018	21.09.2018
Image-14	19. 10. 2018	22.10.2018

Figure 2.4 Fused image datasets of Sentnel-1 and Sentinel-2.

The target Coordinate Reference System (CRS) is selected to match the UTM zone of the overlaying Sentinel-2 granules. This processing step is useful to obtain Sentinel-1 GRD products to Sentinel-2 MSI data grids in a common spatial grid for image fusion and co-registration. Finally, the output product is used for further analysis. Figure 2.3 shows the geo-located border figure of Sentinel-1 and 2, RGB image of backscattered VV of Sentinel-1, red and blue band of Sentinel-2 and co-registered image of VV backscattered and red band. The dataset for Sentinel-2 around 0-3 days of the acquisition of Sentinel-1 are used for multimodal image fusion as shown in the list of datasets in figure 2.4. Back scattered VV and VH polarized bands of Sentinel-1 and bands 2-5, 11and 12 of Sentinel-2 are considered for multimodal image analysis. The pixel-based change detection method has special requirement of co-registration accuracy. In earlier report [6] of multispectral datasets FFT co-registration approach [7] was used. In other publication [8] another successful co-registration method known as GeFolki (Geoscience Extended Flow Optical Lucas–Kanade Iterative) [9] was used. The same method (GeFolki) is used here for co-registration of fused image datasets. The co-registration is done in pre-processing step before analysis.

3. CHANGE DETECTION METHOD

In this project the SAR and MS datasets are integrated to estimate the change detection. In earlier two reports [6], [8] the MS and SAR datasets are used separately to estimate infrastructure growth monitoring using statistical approach LRT and GLRT. In this paper change detection estimation based on PCA (Principal Component analysis) approach is also compared with earlier methods.

3.1 Principal component analysis

PCA is a popular dimensionality reduction technique used in Machine Learning applications. The purpose of using a principal component analysis is to reduce the dimensionality of the data. A set of correlated variables is transformed in other uncorrelated variables known as principal components which contain the maximum original information with a physical meaning that needs to be explored.

ITPCA method

Unsupervised change detection analysis using ITPCA (Iterated Principal Component Analysis) [10] is presented here to indicate the continuous change occurring over a long period of time. In ITPCA based change detection analysis the assumption of a linear relation between no-change pixels belonging to the consecutive acquisitions are used [11]. If we consider a bi-temporal feature space for a single spectral band i where each pixel is denoted by a pixel vector $X_i = [x_i(t_1),\ x_i(t_2)]^T$ then two PCA separates all the pixels into two main clusters along the two principal axes. The unchanged pixels are clustered along the first principal axis whereas the changed pixels are far away from and along the second component. The magnitude of 'change' is quantified by the magnitude of the second principal component. Figure 3.1 a) and b) shows the concept of 'no-change' vs 'change' using two PCA components and iterative fitting of no-change axis respectively. PCA components are estimated from eigenvectors of the covariance matrix of all pixels.

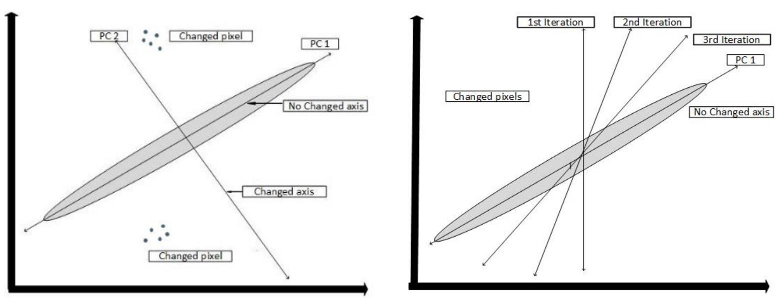

a b

Figure 3.1a) PCA concept of no-change vs change axis, b) Iterative fitting of the no-change axis.

Initial assumption of the method mentioned above, the line identified by the direction of first principal component (pc_1) can be considered as the correlation line between two single band images I_1 and I_2 . Here, the second principal component (pc_2), which is orthogonal to the first, can be used to quantify the change of a given pixel by computing the distance between that pixel and the correlation line. The distance of the second component from the correlation line is used to quantify the change. The main error in this method is the assumption that all pixels are considered for analysis. An iterative scheme is thus used in ITPCA, where the distance between a given pixel and the correlation line computed at a given iteration is used to derive its weight. The pixel which is far away from the correlation line has less probability to be unchanged pixel and have less weight. The iteration weight w_i is represented as the inverse of the magnitude for each pixel p_i for $i = 1, 2, ..m$ can be expressed as:

$$w_i = \frac{1}{\sqrt{|p_{i,2}|}} \tag{1}$$

Where, $p_{1,2}$ is the value computed from second principal component pc_2 . Weights are normalized using the expression:

$$w_i^{'} = \frac{w_i}{\sum_{j=1}^{m} w_j} \text{ such that } \sum_{i=1}^{m} w_i^{'} = 1 \tag{2}$$

Once the correlation line is found by iteration process, its angular coefficient is used to perform calibration between the two images. The analysis is extended to solve the change detection problem for multi band data by applying the approach to all bands independently. The image difference between the calibrated images at each band is found and based on the assumption of Gaussian mixture, three distributions (No-change, Change, ambiguous) are estimated by expectation maximization (EM) algorithm [12], which provides the means and the variances. Thus, only the first principal component, which is the component with the highest variance possible, is considered for the estimation of the Gaussian distribution mixture. The no-change observations are considered to be normally distributed and uncorrelated. Let Z be the sum of the squares of the calibrated image difference X_{Di} and it is represented as:

$$Z = \sum_{i=1}^{N} \left(\frac{X_{Di}}{\sigma_{Di}^{nc}} \right) \tag{3}$$

Where, σ_{Di}^{nc} is the variance of no-change distribution. It follows a χ^2 distribution with N degrees of freedom. The change probability can be defined as follows:

$$\Pr(Change) = P_{\chi^2;N(z)} \tag{4}$$

Where, $P_{\chi^2;N(z)}$ represents the distribution function.

In order to identify the stronger changes there is a need to compute both the threshold between the first and second distributions and the threshold between the second and the third distributions. Both thresholds are used to build the ICM (initial change mask) [13].

The minimization of co-registration error is also addressed considering 8- neighborhood pixels. MATLAB software code developed [10] for change detection of multispectral images using ITPCA method is used as basic code for the analysis. In this case SAR and Multispectral fused images are used for change detection.

3.2 LRT and GLRT method

The LRT and GLRT methods used in earlier publications are described in brief in this section as these change detection methods were used for comparison in this project.

The well-established LRT statistic is used for determining the pixel-wise change in a series of complex covariance matrices of multi-looked polarimetric SAR data. Covariance matrices of the back-scattered vector follows the Gaussian-based complex Wishart distribution. LRT are decomposed into a product of test statistics that test simpler hypothesis by using all the images in series except one at a time. The method and theory were discussed in detail in earlier publication [8].

In GLRT method a statistical model is established from series of MS image data over a long period of time, assuming there is no considerable change during that time period and then compare it with the multispectral image data obtained at a later time. GLRT was used to detect the target (changed pixel) from probabilistic estimated model of the corresponding background clutter (non-changed pixels). The discriminant test is known as 'clairvoyants', and discriminant detectors are known as clairvoyant detectors. GLRT method for change detection of multispectral images were also used in earlier report [6].

4. RESULTS AND ANALYSIS

4.1 ICPTA analysis

Two bands of Sentinel-1(backscattered VV and VH) and six bands (Blue, Green, and Red, Near Infra-Red and SWIR 1 and 2) of Sentinel-2 are geo-collocated and fused together to create a dataset during the time interval of 2015- 2018 for this analysis. Thus, fused datasets of eight bands of 14 different dates as shown in figure 2.4 are used for continuous change detection. ICM (Initial change mask) based approach using PCA linear transformation as described in section 3.1 are used. Figure 4.1 shows the density scatter plots of principal component 1 vs 2 with ICM approach and without ICM. It is noted that incorrect identification of the correlation line in case of without ICM approach. The incorrect correlation line is due to the inclusion of the changed pixels. The spread of the first component is also more which includes changed pixels. Chi-square distribution probability of change maps are shown in figure 4.2. The first change map from August 2015 to October 2016 is shown in the plot. It is very much clear that the change has happened between these two dates. The second plot also shows clearly the change from October 2016 to June 2017.

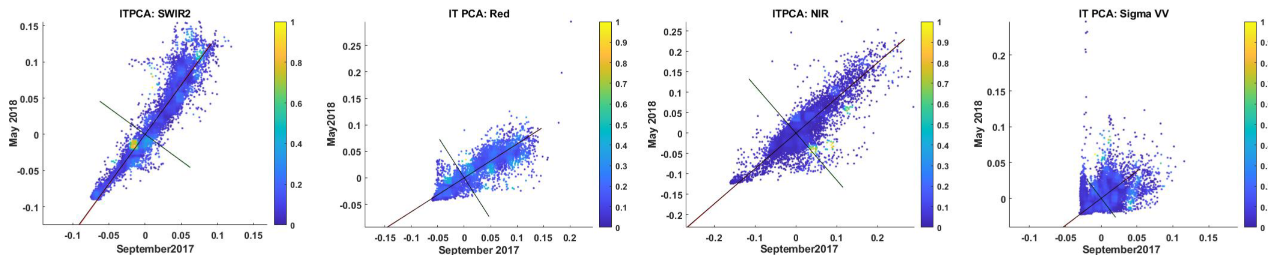

a

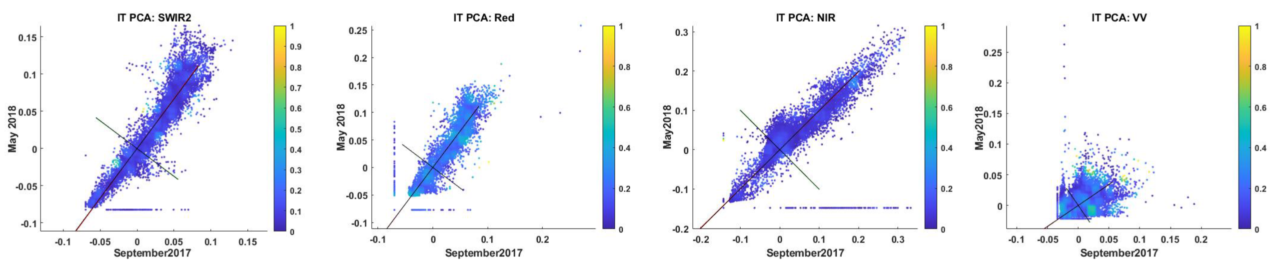

b

Figure 4.1a) Density scatter plots of the SWIR2, Red, NIR and back scattered VV bands with ICM. b) Density scatter plots of the SWIR2, Red, NIR and back scattered VV bands without ICM.

a) **2015 August to 2016 October**

b) **October 2016 to June 2017**

Figure 4.2 chi-square probability of change maps between two dates of datasets.

Figure 4.3 is the total chi-square distribution change map over 10 datasets August 2015 to August 2018. The area under yellow curve is our region of interest. It is the sum of changes over three years estimated from these 10 datasets. Grey shade values shown in colorbar shows how many times the pixels have changed. The second principal components of bi temporal images at different bands are visualized in spectral space in figure 4.4, figure 4.5 and figure 4.6. The second principal components in spectral space shows the changed pixels. False Color Composite (FCC) of second PC of backscattered VV, VH of SAR and red band of MS dataset is shown in figure 4.4 . The second principal component in spectral space from fused datasets shows the VV and VH changed pixels (visualized as blue and green) along with the Red band which is extra information of changed pixels when compared with RGB image of multispectral data as shown in figure 4.5. Similarly, in figure 4.6 the second principal component of NIR, SWIR1 and SWIR2 are plotted which also shows the extra changed pixels in other areas from second PC of RGB image or FCC image of VV, VH and Red bands. Thus second principle component plot in spectral space of all bands shows change in different spectral bands. The change over the year 2015 to 2018 is clearly visible from the images.

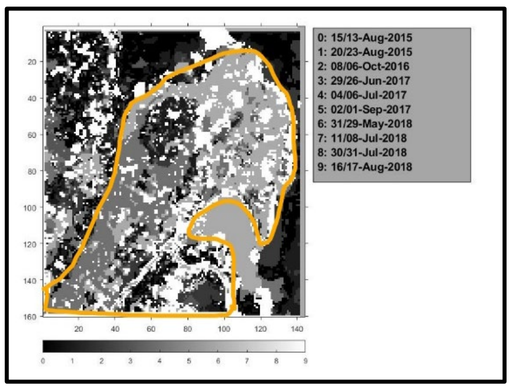

Figure 4.3 Total chi-square probability distribution of change map over 10 datasets from August 2015-August 2018. Region of interest for change is shown using yellow curve.

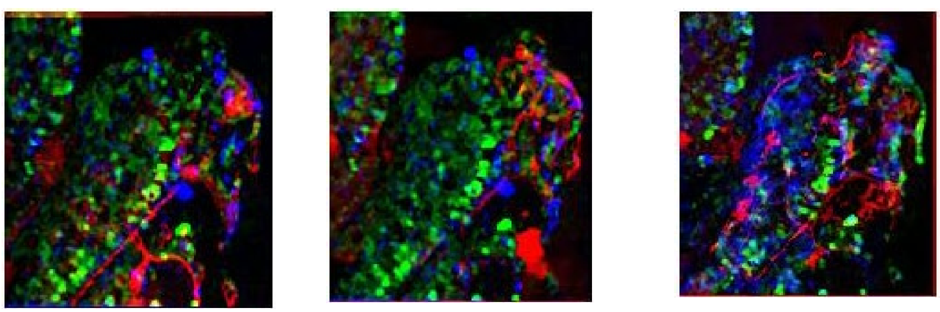

Aug 2015 to Oct 2016 (VV,VH, R)

October 2016 to June 2017 (VV,VH, R)

September 2017 to May 2018 (VV,VH, R)

Figure 4.4 FCC (VV, VH and R) images using second principal components for different datasets.

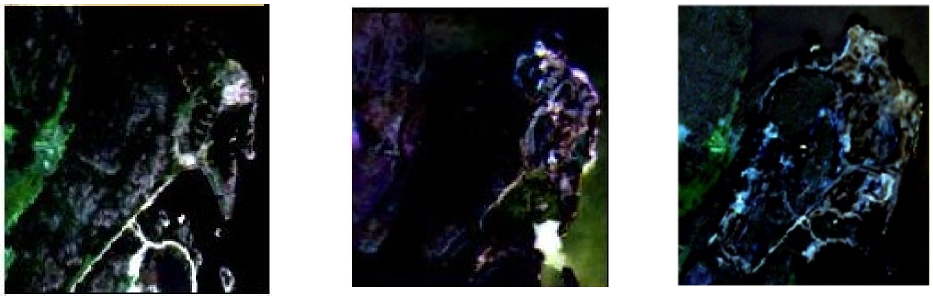

Aug 2015 to Oct 2016 (R,G, B) **October 2016 to June 2017 (R,G, B)** **September 2017 to May 2018 (R,G, B)**

Figure 4.5 RGB change images using second principal components for different datasets.

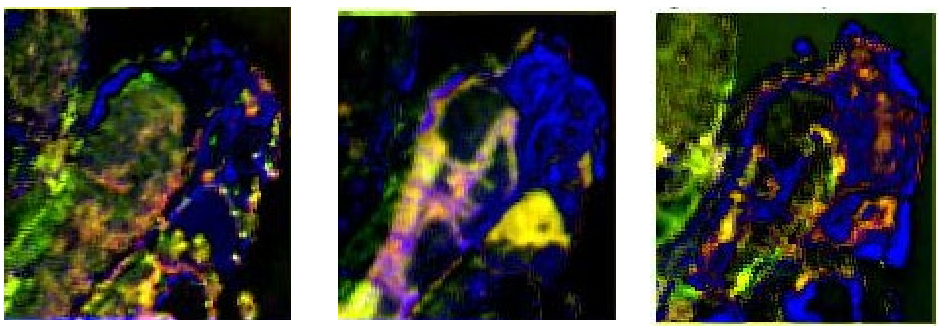

Aug 2015 to Oct 2016 (NIR,SWIR1, SWIR2) **October 2016 to June 2017 (NIR,SWIR1, SWIR2)** **September 2017 to May 2018 (NIR,SWIR1, SWIR2)**

Figure 4.6 FCC (NIR, SWIR1 and SWIR2) images using second principal components for different datasets.

4.2 LRT analysis

In earlier publication [8] the change detection was estimated using multitemporal SAR data from Sentinel-1 over the year 2015-2018. LRT method as briefly explained in 3.2 was used for change detection. Analysis was done in the same region of interest. Approximately 49 datasets during the period of 2015-2018 were downloaded. Before data analysis datasets were pre-processed using the SNAP software for further reduction of speckle noise and terrain correction. Co-registration of the datasets were also done before change detection using LRT method.

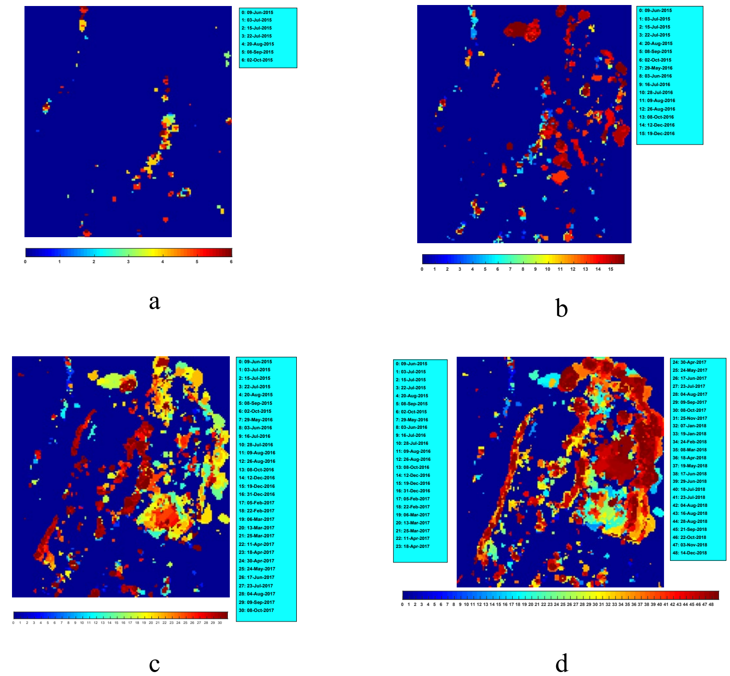

Figure 4.7 Plot of changed pixels in the area of interest a) Year 2015 with 7 datasets, b) Year 2015-2016 with 16 datasets, c) Year 2015-2017 with 31 datasets, d) Year 2015-2018 with 49 datasets. Color indicates pixel changes in particular dates.

Figure 4.7 is the changed pixel plot in different years of the datasets of SAR datasets from Sentinel-1. The color bar corresponds to the dates of the datasets. The color code corresponds to changed pixels in different dates of each year plotted in same image with zero corresponding to the base date i.e. 9th June, 2015. All comparisons shown in the figure 4.7 are made with respect to the base date. It is obvious from the plot that the changed pixels are more in 2017 and 2018 than in the year 2015 or during the first half of the year of 2016. It is pixel based change analysis considering a threshold value of probability. If the probability of change is greater than the threshold then it is considered that the pixel is changed.

4.3 GLRT analysis

GLRT method is briefly explained in section 3.2. In earlier project [6] the results and analysis using GLRT method and Multispectral images over the same region are shown in detail. Here the results and analysis are shown for comparison. In case of multispectral images the datasets are downloaded for Sentinel-2 and Landsat-8 by defining same area of interest. The datasets were pre-processed and co-registered before analysis. Some of the datasets, depending on time of the year, had more cloud coverage. Especially if the area of interest was mostly covered by clouds then it had to be rejected for processing. This is the major disadvantage of multispectral images over SAR images.

Figure 4.8 is the GLRT result of changed pixels plot from Sentinel-2 and Landsat-8 datasets during different dates of the year 2017. The comparison with results of Sentinel-1and Landsat-8 shows clearly the change detection is in the same region of interest. The fourth image in part b) of figure 4.8 has a part covered with clouds and it is not at all of good quality for processing. In spite of that, it shows some detected changed pixels over the region of interest selected, shown by red circles. Lastly figure 4.9 is an example of Sentinel-2 and Landsat-8 image at same year and approximately within a gap of four months. Comparison between them visually shows that some detected changed pixels are nearly over the same area.

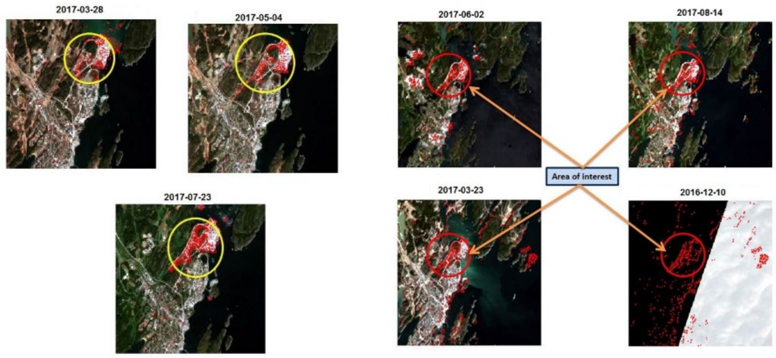

a b

Figure 4.8 The changed pixels shown as red squares in different dates as a result of GLRT test in

a) Sentinel-2 datasets, b) Landset-8 datasets.

Figure 4.9 The detected changed pixels shown both in Sentinel-2 and Landsat-8 in approximately four months gap.

5. CONCLUSIONS

This paper presents the change detection analysis over a period of time using ITPCA method and SAR and Multispectral fused datasets. It is difficult to have both SAR and Multispectral datasets of Sentinel-1 and Sentinel-2 at same instant or same day. Therefore, the datasets within three days of interval of time are fused together taking into consideration that there is no considerable change in the images. The change detection is pixel by pixel. ITPCA method has advantage over general PCA that it includes only unchanged pixels for correctness of principal component analysis. The multimodal technique has the advantage of extra exploitation from remote sensing sensors in joint use such as SAR and multispectral. SAR spectral bands measure physical properties and can be acquired independently without daylight conditions. RGB and other spectral bands like NIR and SWIR measure chemical characteristics but need cloudless sky and daylight. The second principal component plots in spectral space (VV,VH and RGB, NIR, SWIR1 and 2) for two pair of images shows the changed pixel map over the period of time. The probability distribution of change maps considering chi-square distribution of difference of images also shows the continuous change over time. The change detection analysis results from earlier publications using LRT and GLRT methods and SAR and Multispectral images are also shown in this paper for comparison. From the analysis it is evident that change detection maps are similar in the same region of interest. It can be concluded the principle component analysis for change detection for multimodal multitemporal datasets has promising potential for further development.

REFERENCES

[1] S. Kotkar and B. Jadhav, "Analysis of various change detection techniques using satellite images," in *2015 International Conference on Information Processing (ICIP)*, Pune,India, 2015.

[2] I.R.Hegazy and M.R.Kaloop, "Monitoring urban growth and land use change detection with GIS and remote sensing techniques in Daqahlia governorate Egypt," *International Journal of Sustainable Built Environment,* vol. 4, no. 1, pp. 117-124, 2015.

[3] H. Ghassemian, "A review of remote sensing image fusion methods," *Information Fusion,* vol. 32, no. Part A, pp. 75-89, 2016.

[4] "Copernicus Open Access Hub," [Online]. Available: https://scihub.copernicus.eu/dhus/#/home.

[5] F. Filipponi, "Sentinel-1 GRD Preprocessing Workflow," in *The 3rd International Electronic Conference on Remote Sensing*, 2019.

[6] U. Datta, "Infrastructure Change Monitoring Using Multitemporal Multispectral Satellite Images," *International Journal of Civil and Architectural Engineering,* vol. 14, no. 5, pp. 155-160, 2020.

[7] M.Guizar-Sicairos, S.T.Thurman and J.R.Fienup, "Efficient subpixel image registration algorithm," *OPTICS LETTERS,* vol. 33, no. 2, pp. 156-158, 2008.

[8] U. Datta, "Infrastructure monitoring using SAR and multispectral multitemporal images," in *Proc. SPIE 11533, Image and Signal Processing for Remote*, 20th September,2020.

[9] A. Plyer, E. Colin-Koeniguer and F. Weissgerber, "A New Coregistration Algorithm for Recent Applications on Urban SAR Images," *IEEE Geoscience and Remote Sensing Letters,* vol. 12, no. 11, pp. 2198-2202, 2015.

[10] N. Falco, P. Marpu and J. Benediktsson, "A toolbox for unsupervised change detection analysis," *International Journal of Remote Sensing,* vol. 37, pp. 1505-1526, 2016.

[11] R. S. Wiemker, D. Kulbach, H. Spitzer and B. Johann, "Unsupervised Robust Change Detection on Multispectral Imagery Using Spectral and Spatial Features," in *Proceedings of the Third International Airborne Remote Sensing Conference and Exhibition*, Copenhagen, Denmark, 1997.

[12] Y. B. Bazi and F. Melgani, "Image Thresholding Based on the EM Algorithm and the Generalized Gaussian Distribution," *Pattern Recognition,* vol. 40, no. 2, p. 619–634, 2007.

[13] N. Falco, P. Marpu and J. A. Benediktsson., "Comparison of ITPCA and IRMAD for automatic change detection using initial change mask," *IEEE International Geoscience and Remote Sensing Symposium,* pp. 6769-6772, 2012.